



Achievable Rates of Underwater Acoustic OFDM Systems over Highly Dispersive Channels

François-Xavier Socheleau, Milica Stojanovic, Christophe Laot, Jean-Michel
Passerieux

► To cite this version:

François-Xavier Socheleau, Milica Stojanovic, Christophe Laot, Jean-Michel Passerieux. Achievable Rates of Underwater Acoustic OFDM Systems over Highly Dispersive Channels. European Conference on Underwater Acoustics, Jul 2012, Edinburgh, United Kingdom. pp.1-8. hal-00697033

HAL Id: hal-00697033

<https://hal.science/hal-00697033v1>

Submitted on 14 May 2012

HAL is a multi-disciplinary open access archive for the deposit and dissemination of scientific research documents, whether they are published or not. The documents may come from teaching and research institutions in France or abroad, or from public or private research centers.

L'archive ouverte pluridisciplinaire **HAL**, est destinée au dépôt et à la diffusion de documents scientifiques de niveau recherche, publiés ou non, émanant des établissements d'enseignement et de recherche français ou étrangers, des laboratoires publics ou privés.

ACHIEVABLE RATES OF UNDERWATER ACOUSTIC OFDM SYSTEMS OVER HIGHLY DISPERSIVE CHANNELS

F.-X. Socheleau	ENSTA Bretagne, UMR CNRS 6285 Lab-STICC, Ueb, Brest, France
M. Stojanovic	Northeastern University, Boston, USA
C. Laot	Institut Mines-Telecom, Telecom Bretagne, UMR CNRS 6285 Lab-STICC, Ueb, Brest, France
J.-M. Passerieux	Thales Underwater Systems, Sophia Antipolis Cedex, France

1 INTRODUCTION

Finding systems that are robust to the environment, while maintaining acceptable data rates, remains one of the major difficulty faced by underwater acoustic communication (UAC) system designers. However, experiments conducted over the last few years have shown that, even in difficult shallow water channels, it now appears possible to significantly increase the data rate with respect to the achievable performance of current commercial-on-the-shelf (COTS) modems. Among the promising transmission techniques, multi-carrier systems such as OFDM (Orthogonal Frequency Division Multiplexing) [1–4] have generated much interest. This is mainly due to the simplicity of OFDM receivers and to the flexibility offered by such systems.

An assessment of the ultimate performance of OFDM systems appears critical to determine whether such a technique could actually yield a significant breakthrough in UAC. For instance, multi-carrier systems are known to limit the interference at the receiver, which improves the robustness of UAC systems. However, this robustness improvement is generally paid back by the loss of spectral efficiency induced by the use of time and/or frequency guard intervals required to limit the interference. The optimal trade-off between low interference and high spectral efficiency is a key ingredient in OFDM system design that has yet to be found. To obtain a better understanding of the interplay between interference and the achievable transmission rates, we suggest to study the information rate of UA-OFDM systems. The channel capacity, defined as the amount of information that can be transmitted with arbitrarily small error probability, appears as a good figure of merit for performance analysis as it jointly considers interference and spectral efficiency.

Unlike the capacity of other channels, the capacity of the shallow water UAC channel has been seldomly addressed [5–8]. Along the line of [9] and motivated by recent results in information theory [10], this paper investigates achievable rates of underwater acoustic OFDM systems. We consider channels where time and frequency dispersion is high enough that (i) neither the transmitter nor the receiver can have a priori knowledge of the channel state information, and (ii) intersymbol/intercarrier interference (ISI/ICI) cannot be neglected in the information theoretic treatment. Expressions for these rates take into account the “cross-channels” established by the ISI/ICI and are based on lower bounds on mutual information that assume independent and identically distributed input data symbols. In agreement with recent statistical analyses of experimental shallow-water data [11], the channel is modeled as a multivariate Rician fading process with a slowly time-varying mean and with potentially correlated scatterers, which is more general than the common wide-sense stationary uncorrelated scattering model.

This paper is organized as follows. Section 2 is devoted to the presentation of the system model and the main assumptions. Achievable rates of OFDM systems transmitting over UA channels are derived in Section 3. In Section 4, the information rate of OFDM systems transmitting over experimental doubly dispersive UA channels surveyed at sea is numerically assessed. Finally, conclusions are given in Section 5.

2 SYSTEM MODEL

2.1 NOTATION

Throughout this paper, lowercase boldface letters denote vectors, e.g. \mathbf{x} , and uppercase boldface letters denote matrices, e.g., \mathbf{A} . The Hadamard (element-wise) products of two matrices \mathbf{A} and \mathbf{B} is written as $\mathbf{A} \odot \mathbf{B}$. The entries of a matrix \mathbf{A} are denoted by $[\mathbf{A}]_{k,n}$, where the indices k and n start at 0. $\mathbf{B}^{(k,k')}$ designates a submatrix of a block matrix \mathbf{B} . The Kronecker symbol is denoted by $\delta(k)$. We let $\text{diag}(\mathbf{x})$ designate a diagonal square matrix whose main diagonal contains the elements of the vector \mathbf{x} . The inner product between two signals $y(t)$ and $z(t)$ is denoted as $\langle y, z \rangle = \int_{-\infty}^{+\infty} y(t)z^*(t)dt$. Finally, $\mathbb{E}\{\cdot\}$ denotes expectation.

2.2 CHANNEL MODEL

We consider a doubly selective baseband equivalent underwater acoustic channel, modeled as a random linear time-varying system \mathbb{H} that maps input signals $x(t)$ into output signals $y(t)$ according to the I/O relationship

$$y(t) = (\mathbb{H}x)(t) + w(t) = \int_{\tau} h_{\mathbb{H}}(\tau, t)x(t - \tau)d\tau + w(t), \quad (1)$$

where $h_{\mathbb{H}}(\tau, t)$ is the channel impulse response and $w(t)$ denotes the ambient noise. According to recent results on the statistical characterization of UA channels [11], the impulse response is modeled as a *trend stationary* random process so that, for all t, t_1 and $t_2 \in \mathbb{R}$

$$h_{\mathbb{H}}(\tau, t) = \tilde{h}_{\mathbb{H}}(\tau, t) + \bar{h}_{\mathbb{H}}(\tau, t), \quad (2)$$

with

$$\mathbb{E}\{h_{\mathbb{H}}(\tau, t)\} = \bar{h}_{\mathbb{H}}(\tau, t), \quad (3)$$

and

$$\begin{aligned} \mathbb{E}\{(h_{\mathbb{H}}(\tau, t_1) - \mathbb{E}\{h_{\mathbb{H}}(\tau, t_1)\})(h_{\mathbb{H}}(\tau, t_2) - \mathbb{E}\{h_{\mathbb{H}}(\tau, t_2)\})^*\} &= \mathbb{E}\{\tilde{h}_{\mathbb{H}}(\tau, t_1)\tilde{h}_{\mathbb{H}}^*(\tau, t_2)\} \\ &= \mathbb{E}\{\tilde{h}_{\mathbb{H}}(\tau, t)\tilde{h}_{\mathbb{H}}^*(\tau, t + t_2 - t_1)\}. \end{aligned} \quad (4)$$

$\bar{h}_{\mathbb{H}}(\tau, t)$ is called the trend and is a slowly time-varying deterministic component. $\tilde{h}_{\mathbb{H}}(\tau, t)$ is a zero-mean wide-sense stationary random process assumed to be Gaussian. This model describes the UA channel as a multivariate Rician fading process with a slowly time-varying mean. $\bar{h}_{\mathbb{H}}(\tau, t)$ can be interpreted as the contribution of (pseudo) deterministic physical phenomena to channel fluctuations (wave undulation, range/depth dependence, bathymetry changes etc.) and $\tilde{h}_{\mathbb{H}}(\tau, t)$ represents the channel fluctuations attributable to scatterers that result in fast fading. Note that since no particular assumption is made about the correlation of scatterers, the model is very general and includes the WSSUS model as a subset. Without loss of generality, the channel is assumed to be normalized so that

$$\lim_{T \rightarrow \infty} \frac{1}{T} \int_{-\frac{T}{2}}^{\frac{T}{2}} \int_{\tau} \mathbb{E}\{|h_{\mathbb{H}}(\tau, t)|^2\} d\tau dt = 1. \quad (5)$$

We define the channel Rice factor as the power ratio between the deterministic trend and the random component, i.e.,

$$\kappa = \lim_{T \rightarrow \infty} \frac{1}{T} \frac{\int_{-\frac{T}{2}}^{\frac{T}{2}} \int_{\tau} |\bar{h}_{\mathbb{H}}(\tau, t)|^2 d\tau dt}{\int_{\tau} \mathbb{E}\{|\tilde{h}_{\mathbb{H}}(\tau, t)|^2\} d\tau}. \quad (6)$$

The ambient noise $w(t)$ is assumed to be Gaussian and to result from the mixture of four sources : turbulence, shipping, waves and thermal noise with non flat power spectral densities (PSD) denoted by $W(f)$ and given in [8].

2.3 OFDM SIGNAL

OFDM signaling schemes can be described by two Weyl-Heisenberg (WH) sets [12, 13]: the one used at transmission, expressed as

$$(g, T, F) \triangleq \{g_{k,n}(t) = g(t - kT)e^{j2\pi nFt}, \|g\|^2 = 1\}_{k,n \in \mathbb{Z}} \quad (7)$$

and the one used at reception, defined as

$$(\gamma, T, F) \triangleq \{\gamma_{k,n}(t) = \gamma(t - kT)e^{j2\pi nFt}, \|\gamma\|^2 = 1\}_{k,n \in \mathbb{Z}} \quad (8)$$

where $T, F > 0$ are the time and frequency shifts of the prototype function $g(t)$ and $\gamma(t)$. The signaling scheme is here assumed to be (bi)orthogonal, so that

$$\langle g_{k,n}, \gamma_{k',n'} \rangle = \delta(k - k')\delta(n - n'). \quad (9)$$

To ease the readability of the results presented in the sequel, we shall restrict our analysis to orthogonal receive pulses (i.e., $\langle \gamma_{k,n}, \gamma_{k',n'} \rangle = \delta(k - k')\delta(n - n')$).

The transmitted signal is

$$x(t) = \sum_{k=0}^{K-1} \sum_{n=0}^{N-1} x_{k,n} g_{k,n}(t), \quad (10)$$

where N is the number of subcarriers and KT is the approximate duration of the transmitted signal. $x_{k,n}$ denotes the data symbols. Since little is known about the exact structure of optimal signaling under the general constraints listed in the introduction, we restrict our analysis to zero-mean, independent and identically distributed (i.i.d.) symbols. We assume that the average power of the input signals is limited so that

$$\frac{1}{KT} \sum_{k=0}^{K-1} \sum_{n=0}^{N-1} \mathbb{E} \{|x_{k,n}|^2\} = P, \quad (11)$$

where $P < +\infty$ is the maximum average power available. The signal-to-noise ratio (SNR) is then defined as

$$\rho \triangleq \frac{P}{\int_0^B W(f)}, \quad (12)$$

where $B = NF$ denotes the system bandwidth.

At reception, the output signal $y(t)$ is projected onto the set $\{\gamma_{k,n}(t)\}$ to obtain

$$y_{k,n} \triangleq \langle y, \gamma_{k,n} \rangle = \langle \mathbb{H}x, \gamma_{k,n} \rangle + \underbrace{\langle w, \gamma_{k,n} \rangle}_{\triangleq w_{k,n}}. \quad (13)$$

$y_{k,n}$ can be developed as

$$y_{k,n} = \langle \mathbb{H}g_{k,n}, \gamma_{k,n} \rangle x_{k,n} + \sum_{\substack{k'=0 \\ (k',n') \neq (k,n)}}^{K-1} \sum_{n'=0}^{N-1} \langle \mathbb{H}g_{k',n'}, \gamma_{k,n} \rangle x_{k',n'} + w_{k,n}, \quad (14)$$

where the second term on the right-hand side (RHS) of (14) represents the intersymbol and intercarrier interference.

The relation (14) can be compactly expressed as

$$\mathbf{y} = \mathbf{H}\mathbf{x} + \mathbf{w}, \quad (15)$$

where the channel input and output vectors of size $NK \times 1$ are respectively defined by

$$\mathbf{x} \triangleq [\mathbf{x}_0^T \mathbf{x}_1^T \cdots \mathbf{x}_{K-1}^T]^T, \text{ with } \mathbf{x}_k \triangleq [x_{k,0} \ x_{k,1} \cdots x_{k,N-1}]^T,$$

$$\mathbf{y} \triangleq [\mathbf{y}_0^T \mathbf{y}_1^T \cdots \mathbf{y}_{K-1}^T]^T, \text{ with } \mathbf{y}_k \triangleq [y_{k,0} \ y_{k,1} \cdots y_{k,N-1}]^T,$$

and where \mathbf{w} is defined analogously. The $NK \times NK$ channel matrix \mathbf{H} is given by

$$\mathbf{H} \triangleq \begin{pmatrix} \mathbf{H}^{(0,0)} & \cdots & \mathbf{H}^{(0,K)} \\ \vdots & \ddots & \vdots \\ \mathbf{H}^{(K,0)} & \cdots & \mathbf{H}^{(K,K)} \end{pmatrix}, \quad (16)$$

where the matrix block $\mathbf{H}^{(k,k')}$ of size $N \times N$ satisfy

$$\left[\mathbf{H}^{(k,k')} \right]_{n,n'} \triangleq \langle \mathbb{H} g_{k',n'}, \gamma_{k,n} \rangle. \quad (17)$$

Since we do not neglect interference, the matrix \mathbf{H} is not diagonal and can be decomposed as follows

$$\mathbf{H} = \text{diag}(\mathbf{h}) + \mathbf{Z}, \quad (18)$$

where \mathbf{h} is the direct channel vector corresponding to the main diagonal of \mathbf{H} and \mathbf{Z} is the ISI/ICI cross-channel matrix containing the off-diagonal terms of \mathbf{H} .

3 ACHIEVABLE RATES

3.1 DEFINITION

Let $\mathcal{P}_{\mathbf{x}}$ be the set of probability distributions on \mathbf{x} that satisfy the constraints given in (11). The maximum achievable rate for an OFDM system is then given by [14]

$$C = \lim_{K \rightarrow \infty} \frac{1}{KT} \sup_{\mathcal{P}_{\mathbf{x}}} I(\mathbf{y}; \mathbf{x}), \quad (19)$$

where $I(\mathbf{y}; \mathbf{x}) = h_E(\mathbf{y}) - h_E(\mathbf{y}|\mathbf{x})$ is the mutual information between \mathbf{y} and \mathbf{x} with $h_E(\mathbf{y})$ the differential entropy of \mathbf{y} . In the *noncoherent* setting, i.e., without a priori knowledge of the channel state information, the maximum achievable rate is notoriously hard to characterize analytically. However, by evaluating the mutual information $I(\mathbf{y}; \mathbf{x})$ for a specific input distribution, and by relying on the following inequality on mutual information [15]

$$I(\mathbf{y}; \mathbf{x}) \geq I(\mathbf{y}; \mathbf{x}|\mathbf{H}) - I(\mathbf{y}; \mathbf{H}|\mathbf{x}), \quad (20)$$

we can get a lower bound on C that yields an information-theoretic criterion useful for the analysis of UA-OFDM systems. Note that the first term on the RHS of (20) corresponds to the *coherent* information rate under perfect channel knowledge at reception and the second term can be interpreted as a penalty term that quantifies the rate loss due to the lack of channel knowledge.

3.2 LOWER BOUND

Theorem 1 *The maximum achievable rate of an OFDM system with i.i.d. input symbols satisfying the average-power constraint (11) and transmitting over the channel modeled by (2) is lower-bounded as $C^{\text{L1}} \leq C$, where*

$$C^{\text{L1}} = C^{\text{coh}} - \lim_{K \rightarrow \infty} \inf_{0 < \alpha < 1} (P_{\mathbf{h}}(\alpha, K) + P_{\mathbf{Z}}(\alpha)) \quad (21)$$

with C^{coh} the achievable rate of UA-OFDM systems with perfect channel knowledge at reception given by

$$C^{\text{coh}} = \lim_{K \rightarrow \infty} \frac{1}{KT} \mathbb{E}_{\mathbf{H}} \left\{ \log \det \left(\mathbf{I} + \frac{PT}{N} \mathbf{H} \mathbf{H}^\dagger \text{diag}(\mathbf{r}_w)^{-1} \right) \right\}. \quad (22)$$

Here, the entries of the $NK \times 1$ noise power vector \mathbf{r}_w are defined as

$$r_w(n + kK) \triangleq W(nF), \quad n \in [0, N - 1], \quad k \in [0, K - 1]. \quad (23)$$

$P_h(\alpha, K)$ and $P_z(\alpha)$ can be seen as penalty terms that characterize the rate loss due to direct and cross channel uncertainty, respectively. $P_h(\alpha, K)$ is expressed as

$$P_h(\alpha, K) = \frac{1}{KT} \log \det \left(\mathbf{I} + \frac{PT}{N\alpha} \mathbf{R}_h \text{diag}(\mathbf{r}_w)^{-1} \right), \quad (24)$$

where \mathbf{R}_h denotes the covariance matrix of the direct channel vector \mathbf{h} , and $P_z(\alpha)$ satisfies

$$P_z(\alpha) = \frac{1}{T} \sum_{n=0}^{N-1} \log \left(1 + \frac{PT}{N(1-\alpha)r_w(n)} \tilde{\sigma}_{I_n}^2 \right), \quad (25)$$

where $\tilde{\sigma}_{I_n}^2$ is the ISI/ICI power, at subcarrier n , due to the random part of the channel.

Proof: A sketch of the proof can be found in Appendix A. The complete proof is available in [16].

4 NUMERICAL ANALYSIS

Bounds on the information rate applied to experimental doubly dispersive UA channels surveyed at sea are analyzed in this section. Common OFDM systems with rectangular pulse shaping are used as a framework in our investigation. $g(t)$ and $\gamma(t)$ are thus defined as

$$g(t) = \begin{cases} \frac{1}{\sqrt{T}} & \text{if } 0 < t \leq T, \\ 0 & \text{otherwise} \end{cases}, \quad \text{and } \gamma(t) = \begin{cases} \frac{1}{\sqrt{T-T_g}} & \text{if } T_g < t \leq T, \\ 0 & \text{otherwise,} \end{cases} \quad (26)$$

where $T_g = T - 1/F$ denotes the guard time between OFDM symbols.

Two shallow water channels, recorded in Mediterranean sea, are considered. Table 1 summarizes the main characteristics of these channels. Both channels result from sea trials performed by Thales Underwater Systems in the Mediterranean sea off La Ciotat (France) in October 2004. From the raw data and for each channel, the trend $\bar{h}_{\text{H}}(\tau, t)$ is separated from the random component $\tilde{h}_{\text{H}}(\tau, t)$ using the empirical mode decomposition method [11]. The maximum time delay spread is estimated as the difference between the longest and the shortest delay where the average power delay profile exceeds 1% of its maximum value (i.e., taps that are 20 dB below the strongest tap are assumed to result from noise and are artificially set to 0). The maximum Doppler spread is similarly defined from the Doppler power spectrum as the maximum delay spread from the average power delay profile. To compute the various expectations required to evaluate the bound C^{L1} , a large number of channel realizations are generated using the channel stochastic replay approach presented in [11]. The grid parameters T and F are chosen according to the grid-matching rule [10]: $T/F = \tau_{\text{max}}/\nu_{\text{max}}$.

Through the evolution of the achievable rate (21) as a function of TF , Figure 1 shows possible trade-offs between interference minimization and loss of signal-space dimensions. As TF increases, the duration of the guard interval increases as well, which results in a lower interference at reception. However, for large TF , the rate loss due to the use of this interval is predominant over the interference decrease. This figure provides a measure of reassurance that current practice in designing OFDM systems for underwater channels is reasonable. That is, oversizing guard intervals duration (i.e., choosing large TF) compared to the channel maximum delay spread is not much detrimental to the information rate, whereas a too small TF can significantly decrease this rate, especially in highly dispersive channels such as channel (b).

Figure 2 shows the achievable rate C^{L1} as a function of the SNR ρ . It suggests that significant rate improvements are possible compared to state-of-the-art UA-OFDM systems. For instance, reliable OFDM transmissions at 2 to 4 bits/sec/Hz are achievable provided an average signal-to-noise ratio of 15 to 20 dB, whereas in the same SNR range, single-input single-output UA-OFDM systems usually operate with a spectral efficiency around 1 bits/sec/Hz [1–3].

Table 1: Summary of at sea experiments

	Channel (a)	Channel (b)
Center frequency (kHz)	6	6
Bandwidth (kHz)	1	1
Distance (m)	2500	5000
Water depth (m)	60-120	60-120
τ_{\max} (ms)	35	47
ν_{\max} (Hz)	2.7	3.2
κ (dB)	4.9	1.6

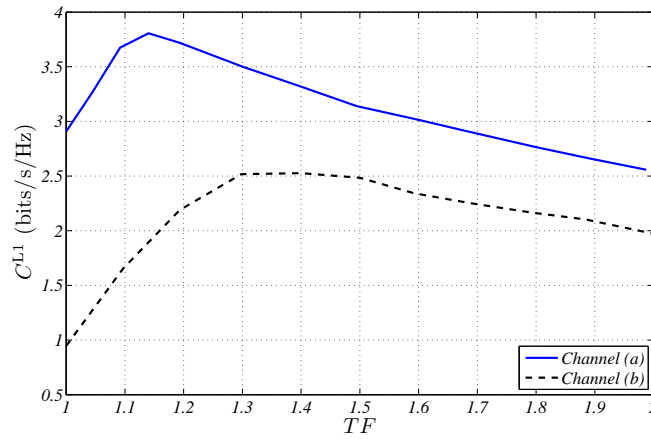


Figure 1: Lower bound C^{L1} as a function of TF , $\rho = 15$ dB.

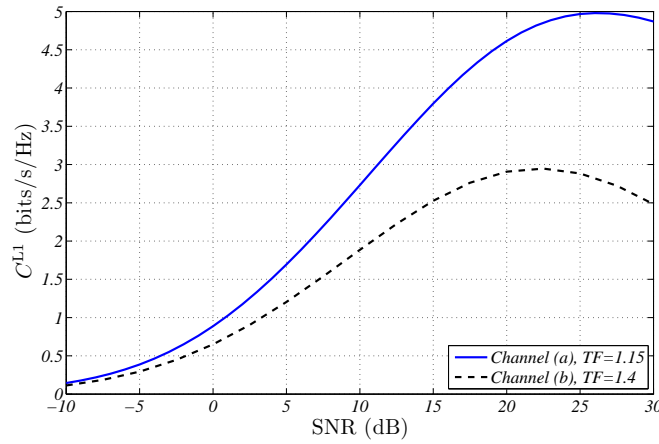


Figure 2: Lower bound C^{L1} as a function of the SNR ρ .

5 CONCLUSIONS

The information-theoretic analysis provided in this paper allow us to obtain a better understanding of the ultimate performance achievable by UA OFDM systems. Numerical assessments on real UA channels with spreading factors (product between the delay and Doppler spread) around 10^{-2} show that reliable OFDM transmissions at 2 to 4 bits/sec/Hz are achievable provided an average signal-to-noise ratio (SNR) of 15 to 20 dB (more details and results can be found in [16]). Although quite

realistic, the system model used in this paper could be more constrained. In particular, to strengthen our results it would be interesting to add a peak-power limitation to our model. It is well known that OFDM systems can be sensitive to this limitation when power amplifier do not operate with a large back-off.

APPENDIX A

A lower bound on C can be obtained by evaluating the mutual information $I(\mathbf{y}; \mathbf{x})$ for a specific input distribution. Specifically, \mathbf{x} is chosen such that $\mathbf{x} \sim \mathcal{CN}(0, \frac{PT}{N}\mathbf{I})$. The proof of Theorem 1 next relies on the following information theoretic inequality [15, 17]:

$$I(\mathbf{y}; \mathbf{x}) \geq I(\mathbf{y}; \mathbf{x}|\mathbf{H}) - I(\mathbf{y}; \mathbf{H}|\mathbf{x}). \quad (27)$$

COMPUTATION OF $I(\mathbf{y}; \mathbf{x}|\mathbf{H})$

The random vectors involved in the computation of $I(\mathbf{y}; \mathbf{x}|\mathbf{H}) = h_E(\mathbf{y}|\mathbf{H}) - h_E(\mathbf{y}|\mathbf{x}, \mathbf{H})$ being all Gaussian, using standard results on entropy it can be shown that

$$I(\mathbf{y}; \mathbf{x}|\mathbf{H}) = \mathbb{E}_{\mathbf{H}} \left\{ \log \det \left(\mathbf{I} + \frac{PT}{N} \mathbf{H} \mathbf{H}^\dagger \text{diag}(\mathbf{r}_w)^{-1} \right) \right\}, \quad (28)$$

COMPUTATION OF $I(\mathbf{y}; \mathbf{H}|\mathbf{x})$

The off-diagonal elements of \mathbf{H} being generally non-null in highly dispersive environments, the derivation of $I(\mathbf{y}; \mathbf{H}|\mathbf{x})$ is not as easy. To obtain the result stated in Theorem 1, \mathbf{y} is first split into an interference-free part and an interference-only part, and then, $I(\mathbf{y}; \mathbf{H}|\mathbf{x})$ is upper-bounded. More precisely,

$$\mathbf{y} = \underbrace{\mathbf{h} \odot \mathbf{x} + \mathbf{w}_1}_{\triangleq \mathbf{y}_1} + \underbrace{\mathbf{Z}\mathbf{x} + \mathbf{w}_2}_{\triangleq \mathbf{y}_2}, \quad (29)$$

where \mathbf{w}_1 are two independent random vectors such that $\mathbf{w}_1 \sim \mathcal{CN}(0, \alpha \times \text{diag}(\mathbf{r}_w))$ and $\mathbf{w}_2 \sim \mathcal{CN}(0, (1 - \alpha) \times \text{diag}(\mathbf{r}_w))$, with $0 < \alpha < 1$. By invoking the chain rule and the data processing inequality, it can be shown that

$$I(\mathbf{y}; \mathbf{H}|\mathbf{x}) \leq I(\mathbf{y}_1; \mathbf{h}|\mathbf{x}) + I(\mathbf{y}_2; \mathbf{Z}|\mathbf{x}). \quad (30)$$

Using that \mathbf{y}_1 is Gaussian given \mathbf{h} and \mathbf{x} , and as a consequence of Jensen's inequality, $I(\mathbf{y}_1; \mathbf{h}|\mathbf{x})$ can be upper-bounded as

$$I(\mathbf{y}_1; \mathbf{h}|\mathbf{x}) \leq \log \det \left(\mathbf{I} + \frac{PT}{N\alpha} \mathbf{R}_{\mathbf{h}} \text{diag}(\mathbf{r}_w)^{-1} \right), \quad (31)$$

where $\mathbf{R}_{\mathbf{h}}$ denotes the covariance matrix of the direct channel vector \mathbf{h} .

$\mathbf{Z}\mathbf{x}$ being Gaussian given \mathbf{x} , using Hadamard's and Jensen's inequality, $I(\mathbf{y}_2; \mathbf{Z}|\mathbf{x})$ is then upper-bounded as follows

$$I(\mathbf{y}_2; \mathbf{Z}|\mathbf{x}) \leq K \sum_{n=0}^{N-1} \log \left(1 + \frac{PT}{N(1-\alpha)r_w(n)} \tilde{\sigma}_{I_n}^2 \right), \quad (32)$$

where $\tilde{\sigma}_{I_n}^2$ is the ISI/ICI power, at subcarrier n , due to the random part of the channel.

Theorem 1 is then tightened by choosing α that minimizes the penalty term, which concludes the proof.

REFERENCES

1. F. Frassati, C. Lafon, P. Laurent, and J. Passerieux. Experimental assessment of OFDM and DSSS modulations for use in littoral waters underwater acoustic communications. In *Proc. IEEE Oceans'05*, pp. 826–831, Jun. 2005.
2. B. Li, S. Zhou, M. Stojanovic, L. Freitag, and P. Willett. Multicarrier Communication Over Underwater Acoustic Channels With Nonuniform Doppler Shifts. *IEEE J. Ocean. Eng.*, 33(2): pp. 198–209, 2008.
3. C. R. Berger, S. Zhou, J. C. Preisig, and P. Willett. Sparse Channel Estimation for Multicarrier Underwater Acoustic Communication: From Subspace Methods to Compressed Sensing. *IEEE Trans. Signal Process.*, 58(3): pp. 1708 – 1721, 2010.
4. G. Leus and P. A. van Walree. Multiband OFDM for Covert Acoustic Communications. *IEEE J. Sel. Areas Commun.*, 26(9): pp. 1662–1673, 2009.
5. J.-M. Passerieux, F.-X. Socheleau, and C. Laot. Achievable Rates over Doubly Selective Rician-Fading Channels under Peak-Power Constraint. *Submitted to IEEE Trans. Wireless Commun.* (in revision), 2012.
6. J.-M. Passerieux, F.-X. Socheleau, and C. Laot. On the capacity of the Underwater Acoustic Communication Channel under Realistic Assumptions,. In *Proc. IEEE European Wireless*, pp. 1–6, Apr. 2011.
7. T. Hayward and T. Yang. Underwater acoustic communication channel capacity: A simulation study. In *Proc. AIP*, Nov. 2004.
8. M. Stojanovic. On the Relationship Between Capacity and Distance in an Underwater Acoustic Communication Channel. *ACM SIGMOBILE Mobile Computing and Communications Review (MC2R)*, 11(4): pp. 64–43, 2007.
9. C. Polprasert, J. Ritcey, and M. Stojanovic. Capacity of OFDM Systems over Fading Underwater Acoustic Channels. *IEEE J. Ocean. Eng.*, 36(4): pp. 514–524, Oct. 2011.
10. G. Durisi, V. I. Morgenshtern, and H. Bolcskei. Sensitivity of Noncoherent WSSUS Fading Channel Capacity. *submitted to IEEE Trans. Inf. Theory*.
11. F.-X. Socheleau, C. Laot, and J.-M. Passerieux. Stochastic Replay of non-WSSUS Underwater Acoustic Communication Channels Recorded at Sea. *IEEE Trans. Signal Process.*, 59(10): pp. 4838–4849, 2011.
12. P. Jung and G. Wunder. The WSSUS Pulse Design Problem in Multicarrier Transmission. *IEEE Trans. Commun.*, 55(10): pp. 1918–1928, 2007.
13. W. Kozek and A. F. Molisch. Nonorthogonal pulses shapes for multicarrier communications in doubly dispersive channels. *IEEE J. Select. Areas Commun.*, 16(8): pp. 1579–1589, 1998.
14. D. Schaffhuber, H. Bolcskei, and G. Matz. System capacity of wideband OFDM communications over fading channels without channel knowledge. In *Proc. IEEE ISIT*, 2004.
15. X. Deng and A. Haimovich. Achievable rates over time-varying rayleigh fading channels. *IEEE Trans. on Commun.*, 55(7), July 2007.
16. F.-X. Socheleau, M. Stojanovic, C. Laot, and J.-M. Passerieux. Information-Theoretic Analysis of Underwater Acoustic OFDM Systems in Highly Dispersive Channels. *Journal of Electrical and Computer Engineering (to appear)*, 2012.
17. V. Sethuraman and B. Hajek. Capacity per unit energy of fading channels with a peak constraint. *IEEE Trans. Inf. Theory*, 51(9), 2005.